Intermolecular potential energy surface and thermophysical properties of the CH4–N2 system

Robert Hellmann, Eckard Bich, Eckhard Vogel, and Velisa Vesovic

Citation: The Journal of Chemical Physics **141**, 224301 (2014); doi: 10.1063/1.4902807
View online: http://dx.doi.org/10.1063/1.4902807
View Table of Contents: http://scitation.aip.org/content/aip/journal/jcp/141/22?ver=pdfcov
Published by the AIP Publishing

Intermolecular potential energy surface and thermophysical properties of the CH_4–N_2 system

Robert Hellmann,[1,a)] Eckard Bich,[1] Eckhard Vogel,[1] and Velisa Vesovic[2]
[1]*Institut für Chemie, Universität Rostock, 18059 Rostock, Germany*
[2]*Department of Earth Science and Engineering, Imperial College London, London SW7 2AZ, United Kingdom*

(Received 21 October 2014; accepted 14 November 2014; published online 8 December 2014)

A five-dimensional potential energy surface (PES) for the interaction of a rigid methane molecule with a rigid nitrogen molecule was determined from quantum-chemical *ab initio* calculations. The counterpoise-corrected supermolecular approach at the CCSD(T) level of theory was utilized to compute a total of 743 points on the PES. The interaction energies were calculated using basis sets of up to quadruple-zeta quality with bond functions and were extrapolated to the complete basis set limit. An analytical site-site potential function with nine sites for methane and five sites for nitrogen was fitted to the interaction energies. The PES was validated by calculating the cross second virial coefficient as well as the shear viscosity and binary diffusion coefficient in the dilute-gas limit for CH_4–N_2 mixtures. An improved PES was obtained by adjusting a single parameter of the analytical potential function in such a way that quantitative agreement with the most accurate experimental values of the cross second virial coefficient was achieved. The transport property values obtained with the adjusted PES are in good agreement with the best experimental data. © *2014 AIP Publishing LLC*. [http://dx.doi.org/10.1063/1.4902807]

I. INTRODUCTION

For low-density gases, the thermophysical properties are governed solely by binary interactions and therefore by the intermolecular pair potentials. Provided that the pair potentials are available, it is possible to calculate the second virial coefficients and transport properties in the dilute-gas limit using statistical thermodynamics and the kinetic theory of gases,[1] respectively. One requires the intermolecular potential energy surfaces (PESs) to be determined using high-level quantum-chemical *ab initio* methods for the calculations to be accurate. For small molecules, such calculations are nowadays routinely carried out, and accurate pair potentials exist for, among others, methane,[2] water,[3] hydrogen sulfide,[4] hydrogen,[5] nitrogen,[6] carbon dioxide,[7] and ethylene oxide.[8] Thermophysical properties have also been calculated for a number of these PESs.[2,4,6–11]

In this work, we extend our recent studies of pure gases[2,4,6–11] to binary CH_4–N_2 mixtures. This system is sufficiently simple, on a molecular level, that the calculation of both the intermolecular PESs and of the thermophysical properties is computationally feasible. Although intermolecular potentials of two unlike polyatomic molecules have been reported previously, this is the first time that transport properties of such a system have been evaluated from accurate *ab initio* potentials. Hence, we have an opportunity to validate the kinetic theory expressions for mixtures, which up to now have always been used in an approximate form. Furthermore, the accurate knowledge of thermophysical properties of CH_4–N_2 mixtures is of interest in different fields ranging from planetary science to oil and gas. Nitrogen and methane are the main constituents of Titan's atmosphere, and the dynamic interaction between the lakes and the atmosphere is currently of special interest.[12–16] Natural gas, which is predominantly methane, also contains nitrogen, which not only reduces its calorific value, but plays an important part in the liquefaction process.

In the dilute-gas limit, the thermophysical properties of CH_4–N_2 mixtures are governed by the CH_4–CH_4, N_2–N_2, and CH_4–N_2 pair potentials. Accurate CH_4–CH_4 and N_2–N_2 potential functions are available and have been used to compute the second virial coefficients and transport properties of the pure gases.[2,6,9,10]

Only three research groups have studied the CH_4–N_2 pair potential using quantum-chemical *ab initio* calculations so far. The potential of Schindler *et al.*[17] is based on supermolecular Hartree-Fock (HF) calculations with basis sets of triple-zeta quality for 21 points on the intermolecular PES. A site-site potential function was fitted to the computed interaction energies. The dispersion interactions, which cannot be described with the HF method, were determined separately by fitting to the cross second virial coefficient $B_{12}(T)$. More recently, Shadman *et al.*[18] computed 204 points on the PES at the MP2 level of theory with basis sets up to aug-cc-pVQZ[19,20] and extrapolated the resulting interaction energies to the complete basis set (CBS) limit. However, they only fitted simple isotropic potential functions to the interaction energies. The most recent investigation of the CH_4–N_2 molecule pair was conducted by Kalugina *et al.*[21] They computed 700 points at the CCSD(T)[22] level of theory with the aug-cc-pVTZ basis set,[19,20] but did not attempt to fit an analytical potential function for the whole PES.

In this paper, a new CH_4–N_2 pair potential is presented. It is based on supermolecular CCSD(T) calculations for 743

a)Electronic mail: robert.hellmann@uni-rostock.de

points on the PES. Basis sets up to aug-cc-pVQZ[19,20] with bond functions have been applied, and the resulting interaction energies have been extrapolated to the CBS limit. A site-site potential function is used to represent the PES analytically. The new potential function has been tested by computing thermophysical properties of dilute CH_4–N_2 gas mixtures. The cross second virial coefficient has been calculated utilizing the Mayer-sampling Monte Carlo (MSMC) approach.[23] The analytical potential function has been further improved by performing an empirical adjustment using the most accurate experimental data for the cross second virial coefficient as guidance. Transport properties in the dilute-gas limit have been determined by means of the classical trajectory approach in conjunction with the kinetic theory of molecular gases.[1,24–30] The accuracy and usefulness of this approach has been demonstrated for several pure molecular gases and atom-molecule gas mixtures.[4,6–11,31–33] In this paper, we limit our investigation of the transport properties to the shear viscosity and the binary diffusion coefficient. Results for the thermal conductivity will be reported separately, as they involve new theoretical developments that go beyond a simple validation of the intermolecular potential. The calculation of the thermophysical properties was performed in the temperature range 70 K to 1200 K. The lower limit was chosen to mimic the lowest temperatures on Titan and thus allow for applications in planetary studies.

In Sec. II, the *ab initio* calculations for the CH_4–N_2 molecule pair and the analytical potential function are described. In Sec. III, the calculation of the cross second virial coefficient is discussed, and the results are compared with experimental data. The methodology for the calculation of the transport properties is presented in Sec. IV, and the results are again compared with experimental data. Summary and conclusions are given in Sec. V.

II. INTERMOLECULAR POTENTIAL

A. *Ab initio* calculations

For all *ab initio* calculations, the CH_4 and N_2 molecules were treated as rigid rotors. In accordance with previous work on the CH_4–CH_4 and N_2–N_2 potentials,[2,6] we used a C–H bond length of 1.0990 Å and a N–N bond length of 1.1014 Å. These values correspond to the zero-point vibrationally averaged geometries, see Refs. 2 and 6 for details. Within the rigid-rotor approximation, each configuration of the two molecules can be expressed by the distance R between the centers of mass of molecule 1 (CH_4) and molecule 2 (N_2) and the four Euler angles θ_1, ψ_1, θ_2, and ϕ. Details concerning the precise definition of these angles can be found in the supplementary material.[34]

Altogether 43 distinct angular configurations and 18 center-of-mass separations between 2.0 Å and 10.0 Å were considered, leading to 774 (43 × 18) configurations, 23 of which were discarded because of excessive molecular overlap at small distances. For eight further configurations in the highly repulsive region of the PES, the quantum-chemical computations failed due to near linear dependencies in the basis sets used.

The interaction energies $V(R, \theta_1, \psi_1, \theta_2, \phi)$ were calculated utilizing the supermolecular approach including the full counterpoise correction[35] at the frozen-core CCSD(T) level of theory with the aug-cc-pVXZ basis sets with $X = 3$ and $X = 4$.[19,20] Both basis sets were supplemented by a small $3s3p2d1f$ set of bond functions located midway along the R axis with exponents of 0.1, 0.3, and 0.9 for s and p, 0.25 and 0.75 for d, and 0.45 for f. The correlation contribution to the interaction energy, $V_{\mathrm{CCSD(T)\,corr}}$, was extrapolated to the CBS limit using the two-point scheme proposed by Halkier *et al.*,[36]

$$V_{\mathrm{CCSD(T)\,corr}}(X) = V^{\mathrm{CBS}}_{\mathrm{CCSD(T)\,corr}} + \alpha\, X^{-3}. \tag{1}$$

Extrapolation of the HF contribution was not necessary, since it converges much faster to the CBS limit than the correlation contribution. Therefore, we used the HF interaction energies from the aug-cc-pVQZ computations to approximate the CBS limit.

The results of the quantum-chemical *ab initio* calculations for all 743 configurations can be found in the supplementary material.[34] The Mainz-Austin-Budapest version of ACES II[37] and its successor CFOUR[38] were employed for all *ab initio* calculations.

B. Analytical potential function

A site-site potential function with nine sites for CH_4 and five sites for N_2 was fitted to the computed interaction energies. Each individual site-site interaction is represented by

$$V_{ij}(R_{ij}) = A_{ij}\exp(-\alpha_{ij}R_{ij}) - f_6(b_{ij}, R_{ij})\frac{C_{6ij}}{R_{ij}^6} - f_8(b_{ij}, R_{ij})\frac{C_{8ij}}{R_{ij}^8} + \frac{q_i q_j}{R_{ij}}, \tag{2}$$

where R_{ij} is the distance between site i in the CH_4 molecule and site j in the N_2 molecule. The damping functions f_n are given by[39]

$$f_n(b_{ij}, R_{ij}) = 1 - \exp(-b_{ij}R_{ij})\sum_{k=0}^{n}\frac{(b_{ij}R_{ij})^k}{k!}. \tag{3}$$

The total intermolecular potential is obtained as the sum over all site-site interactions,

$$V(R, \theta_1, \psi_1, \theta_2, \phi) = \sum_{i=1}^{9}\sum_{j=1}^{5} V_{ij}[R_{ij}(R, \theta_1, \psi_1, \theta_2, \phi)]. \tag{4}$$

The positions and partial charges q_i and q_j of the sites in the two molecules were taken from previous work on the CH_4–CH_4 and N_2–N_2 potentials.[2,6] In the CH_4 molecule, there is one site on the carbon atom, one on each of the four C–H bonds at a distance of about 0.97 Å from the carbon atom, and one opposite to each hydrogen atom at a distance of about 0.73 Å from the carbon atom. In the N_2 molecule, one site is at the center of mass, and the other four are near the nitrogen atoms at distances of about 0.45 Å and 0.68 Å from the center of mass. Hence, there are three different types of sites in each molecule and nine types of site-site interactions. The

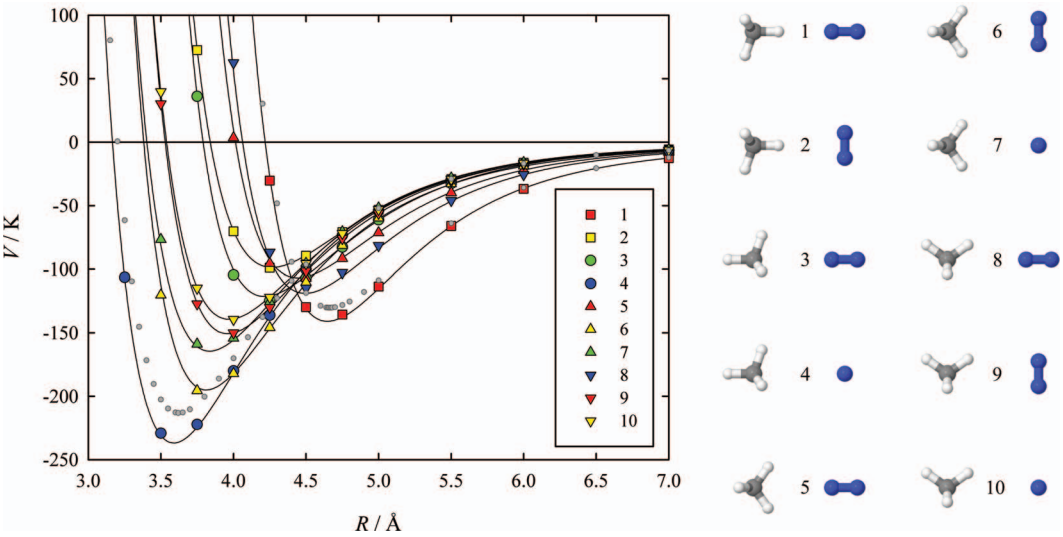

FIG. 1. CH_4–N_2 pair potential as a function of the distance R for 10 of the 43 considered angular configurations. The *ab initio* calculated values are represented by colored symbols and the fitted analytical potential function by solid lines. The small gray circles represent the values obtained by Kalugina *et al.* (Ref. 21) for angular configurations 1 and 4.

parameters A, α, b, C_6, and C_8 for these nine types of interactions were optimized in a nonlinear least-squares fit to the 743 *ab initio* interaction energies. The C_6 parameters were constrained so that the isotropic average of the C_6 dispersion coefficient for CH_4–N_2, $C_{6\,\mathrm{iso}} = \sum_{i=1}^{9} \sum_{j=1}^{5} C_{6\,ij}$ is equal to the accurate value of 96.94 a.u.[40] obtained from dipole oscillator strength distributions (DOSDs).

Figure 1 shows the distance dependence of the *ab initio* calculated values and of the fitted analytical potential function for 10 of the 43 considered angular configurations. The interaction energies are given in Kelvin, i.e., they have been divided by Boltzmann's constant k_B. In Fig. 2, the fitted interaction energies are plotted against the corresponding *ab initio* values for energies up to 10 000 K. The deviations from a straight line are very small, demonstrating the high quality of the fit. The analytical PES exhibits only one distinct equilibrium structure with $D_e = 237.54$ K. It corresponds very closely to the minimum of angular configuration 4 in Fig. 1. The parameters of the analytical PES and the details of the equilibrium geometry are given in the supplementary material.[34]

In our study of the CH_4–CH_4 potential,[2] we also used the highly accurate CCSD(T) method and the zero-point vibrationally averaged geometry of CH_4 for the calculation of the interaction energies. However, using a vibrationally averaged geometry does not fully account for vibrational effects on the interaction energies. Vibrations strongly influence the polarizability of methane[41,42] and consequently the strength of the dispersion interactions. By increasing the dispersion contribution of the analytical potential function, we achieved satisfactory agreement with experimental data for the second virial coefficient over a wide temperature range.

For the CH_4–N_2 potential of the present paper, it was again necessary to adjust the analytical potential function in order to obtain good agreement with the most accurate experimental data for the cross second virial coefficient (see Sec. III). We tested two different approaches. In the first approach, the C_6 parameter for the interaction between the sites in the centers of mass of the molecules was adjusted, which resulted in an increase of D_e to 245.21 K. In the second approach, we adjusted the C_8 parameter for that particular site-site interaction, resulting in a D_e value of 248.24 K. Both approaches result in nearly identical changes of the cross second virial coefficient for all but the lowest temperatures. The C_8 adjustment should be preferred, since the C_6 site-site parameters were constrained in the fit to yield the accurate DOSD value for $C_{6\,\mathrm{iso}}$. Thus, the potential function with the C_8 adjustment was used for all further calculations.

For completeness, we also compare our PES with the most recently published *ab initio* interaction energies, obtained by Kalugina *et al.*[21] using the CCSD(T) method

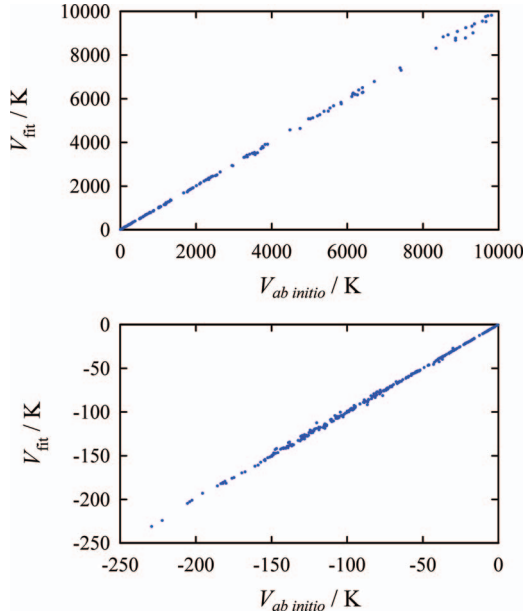

FIG. 2. Interaction energies from the fitted analytical potential function versus the corresponding *ab initio* values.

with the aug-cc-pVTZ basis set. Figure 1 shows their results for two angular configurations. Even without the adjustment of the C_8 dispersion contribution, the present potential features significantly deeper wells. The improvement in our PES can be attributed to the use of larger basis sets, extrapolation to the CBS limit, and the use of vibrationally averaged monomer geometries (as opposed to equilibrium geometries) in the present work.

III. CROSS SECOND VIRIAL COEFFICIENT

The classical cross second virial coefficient for rigid molecules as a function of temperature is given by

$$B_{12}^{\mathrm{cl}} = -\frac{N_{\mathrm{A}}}{2}\int_0^{\infty}\langle f_{12}\rangle_{\Omega_1,\Omega_2} d\mathbf{R}, \tag{5}$$

with

$$f_{12} = \exp\left[-\frac{V(\mathbf{R},\Omega_1,\Omega_2)}{k_{\mathrm{B}}T}\right] - 1. \tag{6}$$

Here, $\mathbf{R}$ is the distance vector between the centers of mass of the two molecules, Ω_1 and Ω_2 represent the angular orientations of molecules 1 and 2, respectively, and the angle brackets denote an average over Ω_1 and Ω_2. To take quantum effects into account, we replaced the intermolecular pair potential V in Eq. (6) by the quadratic Feynman-Hibbs (QFH) effective pair potential,[43] which can be written for the CH_4–N_2 molecule pair as

$$V_{\mathrm{QFH}}(T) = V + \frac{\hbar^2}{24k_{\mathrm{B}}T}\left[\frac{1}{\mu}\left(\frac{\partial^2 V}{\partial x^2}+\frac{\partial^2 V}{\partial y^2}+\frac{\partial^2 V}{\partial z^2}\right) + \frac{1}{I_1}\left(\frac{\partial^2 V}{\partial \psi_{1,a}^2}+\frac{\partial^2 V}{\partial \psi_{1,b}^2}+\frac{\partial^2 V}{\partial \psi_{1,c}^2}\right) + \frac{1}{I_2}\left(\frac{\partial^2 V}{\partial \psi_{2,a}^2}+\frac{\partial^2 V}{\partial \psi_{2,b}^2}\right)\right], \tag{7}$$

where μ is the reduced mass of the molecule pair, x, y, z are the cartesian components of $\mathbf{R}$, I_1 and I_2 are the moments of inertia of molecules 1 (CH_4) and 2 (N_2), the angles $\psi_{1,a}$, $\psi_{1,b}$, $\psi_{1,c}$ correspond to rotations around the principal axes of CH_4, and $\psi_{2,a}$ and $\psi_{2,b}$ are the corresponding angles for N_2.

We used the MSMC approach of Singh and Kofke[23] to compute the cross second virial coefficient for 58 temperatures between 70 K and 1200 K using the hard-sphere fluid with $\sigma = 4.5$ Å as reference system. Results for all temperatures were obtained simultaneously by performing multi-temperature simulations[6,23,44] with a sampling temperature of 70 K and 2×10^{10} trial moves. For each MC trial move, one of the molecules was displaced and rotated. Maximum step sizes for the MC moves were adjusted in short equilibration periods to achieve acceptance rates of 50%. The second derivatives of the pair potential in Eq. (7) were evaluated analytically. Computed virial coefficients from eight independent simulation runs were averaged. The expanded uncertainty (coverage factor $k = 2$) of the Monte Carlo integration is smaller than 0.03 $\mathrm{cm^3\ mol^{-1}}$ for all temperatures.

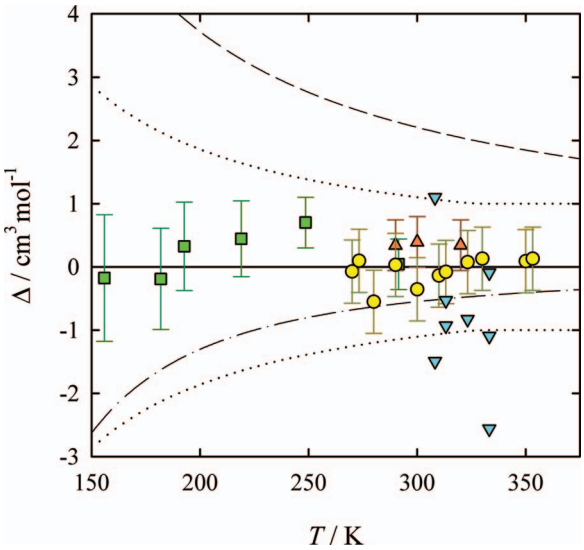

FIG. 3. Deviations, $\Delta = B_{12} - B_{12,\mathrm{adj}}^{\mathrm{QFH}}$, of experimental and calculated values for the cross second virial coefficient of the CH_4–N_2 molecule pair from values obtained with Eq. (8): □, Roe (Ref. 45); △, Martin *et al.* (Ref. 46), reanalyzed; ◯, Jaeschke and Hinze (Ref. 47); ▽, Ababio *et al.* (Ref. 48), reanalyzed; ·····, upper and lower estimated error bounds for $B_{12,\mathrm{adj}}^{\mathrm{QFH}}$; – – –, results for unadjusted potential; — · —, classical results for adjusted potential.

We fitted the following analytical function to the values obtained with the adjusted potential including the QFH correction:

$$\frac{B_{12,\mathrm{adj}}^{\mathrm{QFH}}}{\mathrm{cm^3\ mol^{-1}}} = \sum_{k=-5}^{1} a_k (T^*)^k + \frac{a_{-0.5}}{\sqrt{T^*}}, \tag{8}$$

where $T^* = T/(100\,\mathrm{K})$, $a_{-5} = -9.277$, $a_{-4} = 16.82$, $a_{-3} = -71.45$, $a_{-2} = -13.89$, $a_{-1} = -270.3$, $a_0 = 31.41$, $a_1 = -0.1404$, and $a_{-0.5} = 78.44$. Equation (8) reproduces the calculated values to within $\pm 0.012\,\mathrm{cm^3\ mol^{-1}}$.

In Fig. 3, the present results for the cross second virial coefficient are compared with selected experimental data.[45–48] The data of Jaeschke and Hinze,[47] derived from isothermal pVT measurements with both a Burnett and an optical apparatus, are the most accurate ones with expanded uncertainties ($k = 2$) of 0.5 $\mathrm{cm^3\ mol^{-1}}$. We used these data as reference for the adjustment of the *ab initio* potential function (see Sec. II B). Apart from two data points, the agreement with the values of Jaeschke and Hinze[47] is within ± 0.15 $\mathrm{cm^3\ mol^{-1}}$ for the adjusted potential, whereas for the unadjusted potential deviations up to -2.9 $\mathrm{cm^3\ mol^{-1}}$ are obtained. Most of the data of the other workers were replicated within their claimed uncertainty. The data of Ababio *et al.*,[48] for which no uncertainties are given, exhibit a large scatter compared to the other illustrated data and are not compatible with the data of Jaeschke and Hinze.[47] We note that we have reanalyzed the measurements of Martin *et al.*[46] and Ababio *et al.*[48] using more accurate values[2,6] for the pure-component virial coefficients.

Table I lists the calculated values obtained for both the unadjusted potential (B_{12}^{cl}, B_{12}^{QFH}) and the adjusted potential

TABLE I. Calculated cross second virial coefficients (in $cm^3\ mol^{-1}$) for the CH_4–N_2 molecule pair.

T (K)	B_{12}^{cl}	B_{12}^{QFH}	$B_{12,adj}^{cl}$	$B_{12,adj}^{QFH}$	$u(B_{12,adj}^{QFH})$	T (K)	B_{12}^{cl}	B_{12}^{QFH}	$B_{12,adj}^{cl}$	$B_{12,adj}^{QFH}$	$u(B_{12,adj}^{QFH})$
70	− 482.2	− 454.8	− 513.5	− 482.9	14.0	310	− 13.7	− 13.2	− 15.9	− 15.4	1.1
75	− 416.2	− 395.1	− 441.9	− 418.5	11.7	320	− 11.5	− 11.0	− 13.5	− 13.1	1.0
80	− 364.1	− 347.4	− 385.7	− 367.4	10.0	330	− 9.4	− 9.0	− 11.4	− 10.9	1.0
85	− 322.1	− 308.6	− 340.6	− 325.9	8.6	340	− 7.4	− 7.0	− 9.4	− 8.9	1.0
90	− 287.5	− 276.4	− 303.7	− 291.6	7.6	350	− 5.6	− 5.2	− 7.5	− 7.1	1.0
95	− 258.7	− 249.4	− 272.9	− 262.8	6.7	360	− 3.9	− 3.6	− 5.7	− 5.4	1.0
100	− 234.2	− 226.3	− 246.9	− 238.4	6.0	370	− 2.4	− 2.0	− 4.1	− 3.7	1.0
105	− 213.2	− 206.4	− 224.7	− 217.4	5.5	380	− 0.9	− 0.5	− 2.6	− 2.2	1.0
110	− 195.0	− 189.2	− 205.4	− 199.1	5.0	390	0.5	0.9	− 1.1	− 0.8	1.0
115	− 179.1	− 174.0	− 188.7	− 183.1	4.6	400	1.9	2.2	0.2	0.6	1.0
120	− 165.1	− 160.6	− 173.9	− 169.0	4.2	420	4.3	4.5	2.7	3.0	1.0
130	− 141.6	− 137.9	− 149.1	− 145.3	3.7	440	6.4	6.7	5.0	5.2	1.0
140	− 122.6	− 119.6	− 129.2	− 126.0	3.2	460	8.4	8.6	7.0	7.2	1.0
150	− 106.9	− 104.5	− 112.8	− 110.2	2.9	480	10.1	10.3	8.8	9.0	1.0
160	− 93.9	− 91.8	− 99.2	− 96.9	2.6	500	11.7	11.9	10.4	10.6	1.0
170	− 82.8	− 80.9	− 87.6	− 85.7	2.4	520	13.1	13.3	11.9	12.1	1.0
180	− 73.2	− 71.6	− 77.6	− 76.0	2.2	540	14.4	14.6	13.3	13.4	1.0
190	− 65.0	− 63.6	− 69.0	− 67.6	2.0	560	15.6	15.8	14.5	14.7	1.0
200	− 57.7	− 56.5	− 61.5	− 60.2	1.9	580	16.7	16.9	15.6	15.8	1.0
210	− 51.3	− 50.2	− 54.9	− 53.7	1.7	600	17.7	17.9	16.7	16.8	1.0
220	− 45.7	− 44.7	− 49.0	− 47.9	1.6	650	19.9	20.1	19.0	19.1	1.0
230	− 40.6	− 39.7	− 43.7	− 42.8	1.5	700	21.8	21.9	20.9	21.0	1.0
240	− 36.0	− 35.2	− 39.0	− 38.1	1.5	750	23.3	23.4	22.4	22.5	1.0
250	− 31.9	− 31.2	− 34.7	− 33.9	1.4	800	24.6	24.7	23.8	23.9	1.0
260	− 28.2	− 27.5	− 30.8	− 30.1	1.3	850	25.7	25.8	24.9	25.0	1.0
270	− 24.8	− 24.1	− 27.3	− 26.6	1.3	900	26.6	26.7	25.9	26.0	1.0
280	− 21.7	− 21.1	− 24.1	− 23.4	1.2	1000	28.2	28.2	27.5	27.6	1.0
290	− 18.8	− 18.2	− 21.1	− 20.5	1.1	1100	29.3	29.4	28.7	28.8	1.0
300	− 16.2	− 15.6	− 18.4	− 17.8	1.1	1200	30.2	30.3	29.6	29.7	1.0

($B_{12,adj}^{cl}$, $B_{12,adj}^{QFH}$). The uncertainties for $B_{12,adj}^{QFH}$, which are also listed in the table, were conservatively estimated as follows:

$$u\left(B_{12,adj}^{QFH}\right) = \max\left(\frac{1}{2}\left|B_{12,adj}^{QFH} - B_{12}^{QFH}\right|, 1\ \mathrm{cm^3\ mol^{-1}}\right). \quad (9)$$

As illustrated in Fig. 3, all the data, with the exception of four datum points of Ababio *et al.*,[48] fall within the estimated uncertainty bounds of the calculated values.

IV. TRANSPORT PROPERTIES

A. Theory

The transport properties of dilute gas mixtures can be calculated using the kinetic theory of molecular gases.[1,24–30] For each transport property, a system of linear equations needs to be solved. For the shear viscosity η of a binary mixture consisting of species A and B, the system of equations is given as

$$\sum_{p'q's't'}\left[\bar{S}\begin{pmatrix} p\ q\ s\ t \\ p'q's't' \end{pmatrix}^{(2)}_{AA} X_A^{p'q's't'} + \bar{S}\begin{pmatrix} p\ q\ s\ t \\ p'q's't' \end{pmatrix}^{(2)}_{AB} X_B^{p'q's't'}\right] = \delta_{p2}\delta_{q0}\delta_{s0}\delta_{t0}\, x_A C^{2000},$$

$$\sum_{p'q's't'}\left[\bar{S}\begin{pmatrix} p\ q\ s\ t \\ p'q's't' \end{pmatrix}^{(2)}_{BA} X_A^{p'q's't'} + \bar{S}\begin{pmatrix} p\ q\ s\ t \\ p'q's't' \end{pmatrix}^{(2)}_{BB} X_B^{p'q's't'}\right] = \delta_{p2}\delta_{q0}\delta_{s0}\delta_{t0}\, x_B C^{2000}, \quad (10)$$

where x_A and x_B are the mole fractions, $X_A^{p'q's't'}$ and $X_B^{p'q's't'}$ are the solutions of the equation system, and $C^{2000} = \sqrt{2}$. The coefficients $\bar{S}\left(\begin{smallmatrix} p\ q\ s\ t \\ p'q's't' \end{smallmatrix}\right)^{(k)}_{\alpha\beta}$ are given by

$$\bar{S}\begin{pmatrix} p\ q\ s\ t \\ p'q's't' \end{pmatrix}^{(k)}_{\alpha\beta} = \delta_{\alpha\beta}\sum_\gamma x_\alpha x_\gamma \langle v\rangle_{\alpha\gamma}\bar{\sigma}'\begin{pmatrix} p\ q\ s\ t \\ p'q's't' \end{pmatrix}^{(k)}_{\alpha\gamma} + x_\alpha x_\beta \langle v\rangle_{\alpha\beta}\bar{\sigma}''\begin{pmatrix} p\ q\ s\ t \\ p'q's't' \end{pmatrix}^{(k)}_{\alpha\beta}, \quad (11)$$

where $\langle v\rangle_{\alpha\beta} = (8k_BT/\pi\mu_{\alpha\beta})^{1/2}$ is the average relative thermal speed of molecules of types α and β. The index γ runs over all mixture components. The quantities $\bar{\sigma}'\left(\begin{smallmatrix} p\ q\ s\ t \\ p'q's't' \end{smallmatrix}\right)^{(k)}_{\alpha\beta}$ and $\bar{\sigma}''\left(\begin{smallmatrix} p\ q\ s\ t \\ p'q's't' \end{smallmatrix}\right)^{(k)}_{\alpha\beta}$ are temperature-dependent generalized cross sections.[1,27,30] They are determined by the binary collisions in the gas and are therefore directly related to the pair potentials. In our previous work on pure polyatomic gases, we used the notation of McCourt *et al.*[1] for the generalized cross sections. For mixtures, we find the present notation involving primed and double primed cross sections, due originally to Curtiss,[27]

more convenient. The link between the two is simple, and the interested reader is referred to Ref. 30 for further details. The shear viscosity is obtained as

$$\eta = \frac{1}{2} k_B T \left(x_A X_A^{2000} + x_B X_B^{2000} \right). \tag{12}$$

It is convenient to use Cramer's rule or a linear equation solver to determine the values of X_A^{2000} and X_B^{2000}. To obtain the viscosity in the first-order approximation, we only need to consider a single set of $pqst$ and $p'q's't'$ values in the system of linear equations (10), $[pqst] = [p'q's't'] = [2000]$. In the present work, we employ a third-order approximation that includes the sets [2000], [2010], [2001], [0200], [2020], [2011], [2002], [2100], and [2200]. It is consistent with the third-order approximation recently introduced for pure gases.[7,8]

The use of Cramer's rule to solve the system of linear equations (10) results in the viscosity being expressed in terms of ratios of determinants,[49] a result that in the first-order approximation has traditionally been used by experimentalists to help analyze their data. In doing so, they introduce an interaction viscosity η_{AB}, which is defined by[1]

$$\eta_{AB} = \frac{m_B}{m_A + m_B} \frac{2 k_B T}{\langle v \rangle_{AB} [\sigma'(2000)_{AB} + \sigma''(2000)_{AB}]}, \tag{13}$$

where $\sigma'(2000)_{AB}$ and $\sigma''(2000)_{AB}$ are shorthand for $\bar{\sigma}'\left(\begin{smallmatrix}2000\\2000\end{smallmatrix}\right)^{(2)}_{AB}$ and $\bar{\sigma}''\left(\begin{smallmatrix}2000\\2000\end{smallmatrix}\right)^{(2)}_{AB}$. The interaction viscosity is a useful quantity, as it is independent of mixture composition and only dependent upon the unlike CH_4–N_2 interaction.

The system of linear equations for the binary diffusion coefficient D can be written as

$$\begin{aligned}
&\sum_{q's't'} \left[\widetilde{S}\begin{pmatrix}1q\ s\ t\\1q's't'\end{pmatrix}^{(1)}_{AA} X_{AB}^{1q's't'} + \widetilde{S}\begin{pmatrix}1q\ s\ t\\1q's't'\end{pmatrix}^{(1)}_{AB} X_{BB}^{1q's't'} \right] \\
&\quad = \delta_{q0}\delta_{s0}\delta_{t0} \frac{x_A m_A}{x_A m_A + x_B m_B} C_A^{1000}, \\
&\sum_{q's't'} \left[\widetilde{S}\begin{pmatrix}1q\ s\ t\\1q's't'\end{pmatrix}^{(1)}_{BA} X_{AB}^{1q's't'} + \widetilde{S}\begin{pmatrix}1q\ s\ t\\1q's't'\end{pmatrix}^{(1)}_{BB} X_{BB}^{1q's't'} \right] \\
&\quad = -\delta_{q0}\delta_{s0}\delta_{t0} \frac{x_A m_A}{x_A m_A + x_B m_B} C_B^{1000},
\end{aligned} \tag{14}$$

where m_α is the molecular mass of component α and $C_\alpha^{1000} = (k_B T / m_\alpha)^{1/2}$. The coefficients $\widetilde{S}\left(\begin{smallmatrix}1q\ s\ t\\1q's't'\end{smallmatrix}\right)^{(1)}_{\alpha\beta}$ are related to those introduced in Eq. (11),

$$\begin{aligned}
\widetilde{S}\begin{pmatrix}1q\ s\ t\\1q's't'\end{pmatrix}^{(1)}_{\alpha\beta} &= \bar{S}\begin{pmatrix}1q\ s\ t\\1q's't'\end{pmatrix}^{(1)}_{\alpha\beta} - \delta_{q0}\delta_{s0}\delta_{t0}\delta_{q'0}\delta_{s'0}\delta_{t'0} \\
&\quad \times \frac{x_\beta}{x_\alpha} \left(\frac{m_\beta}{m_\alpha} \right)^{1/2} \bar{S}\begin{pmatrix}1q\ s\ t\\1q's't'\end{pmatrix}^{(1)}_{\alpha\alpha}.
\end{aligned} \tag{15}$$

The product of the molar density and the binary diffusion coefficient, $\rho_m D$, is obtained as

$$\rho_m D = \frac{(x_A m_A + x_B m_B)^2}{m_A m_B} C_A^{1000} X_{AB}^{1000}. \tag{16}$$

In the first-order approximation for $\rho_m D$, the only set of qst and $q's't'$ values used is [000]. Note that in the first-order approximation the binary diffusion coefficient is determined solely by the CH_4–N_2 potential and is independent of the mixture composition. In the second-order approximation, we also include the sets [010], [001], [100], and [200]. This is consistent with the recently published second-order approximation for the self-diffusion coefficient.[33] To obtain a third-order approximation, the sets [020], [011], and [002] are added to those for the second-order approximation.

It is also of interest to examine the relation between the binary diffusion coefficient and the interaction viscosity as a function of temperature. It is customary in kinetic theory to do this by defining the dimensionless parameter A^* as[1,26,49]

$$A^* = \frac{5}{3} \frac{\mu_{AB} \rho_m D}{\eta_{AB}}, \tag{17}$$

where D refers to the binary diffusion coefficient evaluated in the first-order approximation. Hence, A^*, like the interaction viscosity and the first-order approximation to the binary diffusion coefficient, is only a function of the unlike interaction between the CH_4 and N_2 molecules. The studies carried out so far on monatomic[49] and polyatomic species[9,32,50–52] indicate that the value of this parameter is nearly independent of the PES and only weakly dependent on the temperature. These properties have led traditionally to the use of the value of A^* to infer the values of binary diffusion coefficients from measurements of the viscosity of mixtures.[49]

B. Numerical evaluation of the generalized cross sections

The generalized cross sections $\bar{\sigma}'\left(\begin{smallmatrix}p\ q\ s\ t\\p'q's't'\end{smallmatrix}\right)^{(k)}_{CH_4-CH_4}$, $\bar{\sigma}'\left(\begin{smallmatrix}p\ q\ s\ t\\p'q's't'\end{smallmatrix}\right)^{(k)}_{CH_4-N_2}$, $\bar{\sigma}'\left(\begin{smallmatrix}p\ q\ s\ t\\p'q's't'\end{smallmatrix}\right)^{(k)}_{N_2-CH_4}$, $\bar{\sigma}'\left(\begin{smallmatrix}p\ q\ s\ t\\p'q's't'\end{smallmatrix}\right)^{(k)}_{N_2-N_2}$, as well as the corresponding double-primed cross sections were computed by means of classical trajectories using an extended version of the TRAJECT software code.[29] This code was originally written for collisions between two linear rigid rotors using expressions for the generalized cross sections derived by Curtiss.[27] The expressions for two nonlinear rigid rotors were later derived and implemented by Dickinson *et al.*[30] Following their approach, the derivation of the expressions for one linear and one nonlinear rigid rotor is straightforward and was carried out as part of this work.

Classical trajectories describing the collision process of two molecules were obtained for a given total energy, $E = E_{tr} + E_{rot}$, by integrating Hamilton's equations from pre- to post-collisional values (initial and final separation: 500 Å). The total-energy-dependent generalized cross sections can be represented as integrals over the initial states. For each molecule pair, they were calculated for 33 values of E, ranging from 20 K to 30 000 K (CH_4–CH_4), 30 K to 30 000 K (CH_4–N_2), and 15 K to 60 000 K (N_2–N_2), by means of a simple Monte Carlo procedure, in which the initial states were generated utilizing quasi-random numbers. Up to 8×10^6 trajectories were computed at each energy. For low energies, the number of trajectories had to be reduced significantly, because the computational demand to achieve a sufficient accuracy for a

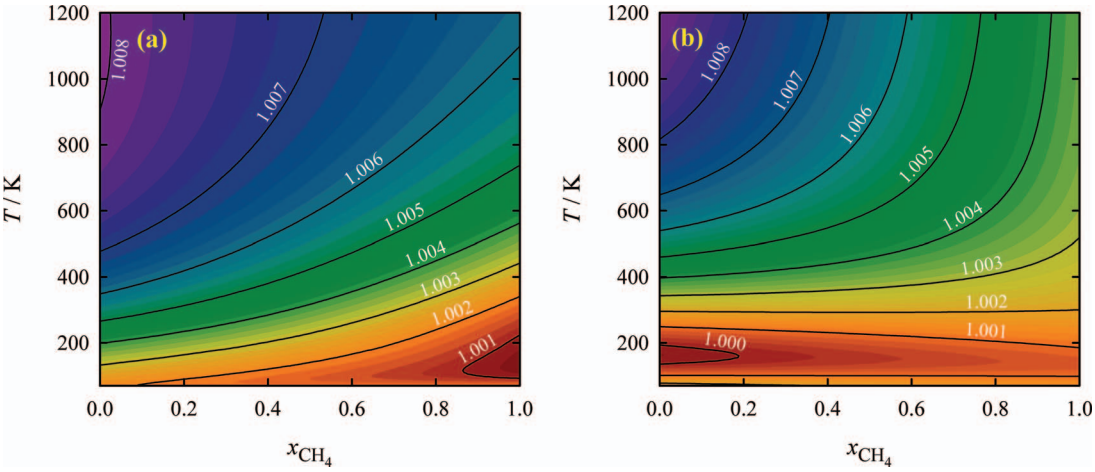

FIG. 4. (a) Ratio of the viscosity in the third-order approximation to that in the first-order approximation. (b) Ratio of the binary diffusion coefficient in the third-order approximation to that in the first-order approximation.

particular trajectory increases as the energy decreases. At the lowest energy for each molecule pair, only 200 000 trajectories were calculated. The final integration over the total energy to obtain temperature-dependent generalized cross sections was performed using Chebyshev quadrature.

C. Results

The values obtained for the shear viscosity and the binary diffusion coefficient using the adjusted intermolecular potential function are given for 155 temperatures between 70 K and 1200 K and 11 mole fractions in the supplementary material.[34] The viscosity values obtained for the pure components are more accurate than the previously published values[6,9] due to the larger number of trajectories employed in the present work and the use of a more accurate third-order approximation for the viscosity. Nevertheless, the differences between the two sets of calculations never exceed 0.1%. The uncertainty of the computed transport property values due to the Monte Carlo integration is estimated to be smaller than 0.1% for all temperatures and mole fractions.

The transport property values obtained with the unadjusted CH_4–N_2 intermolecular potential agree within ±0.1% for temperatures above 400 K with those for the adjusted potential. The deviations increase towards lower temperatures, reaching +0.5% for the shear viscosity and +1.5% for the binary diffusion coefficient of an equimolar mixture at 70 K.

The variation of $\rho_m D$ with composition is small, and it is within ±0.1% for temperatures up to 360 K. At higher temperatures, $\rho_m D$ in the limit of pure N_2 is systematically larger, but the differences are at most 0.5%.

For both transport properties, the relative deviations between the first- and third-order results do not exceed 0.9% as illustrated in Fig. 4. The second- and third-order results differ by less than 0.1% for all temperatures and mole fractions.

The parameter A^*, defined by Eq. (17), exhibits the typical behavior already observed for other polyatomic gases.[9,32,50–52] It increases with temperature from 1.072 at 70 K to 1.155 at 190 K and then remains relatively constant, within 0.5%, reaching a value of 1.158 at 1200 K. Its magnitude, at all temperatures, is between the values for the corresponding pure species, for which A^* is defined in terms of the self-diffusion coefficient and the viscosity.[50]

D. Comparison with experimental data

The viscosity values computed with the adjusted potential function are compared in Fig. 5 with the best available experimental data,[53,54] selected on the basis of low quoted uncertainty and obtained in viscometers with well-defined working equations. Two such data sets were chosen.

Kestin and Ro[53] used an oscillating-disk viscometer to measure the viscosities of pure nitrogen and four mixtures at atmospheric pressure between 298 K and 473 K with claimed uncertainties of less than 0.3%. However, it is known that the viscometer used by Kestin and Ro suffered from a design flaw concerning the temperature measurement using thermocouples, which resulted in viscosity values that are

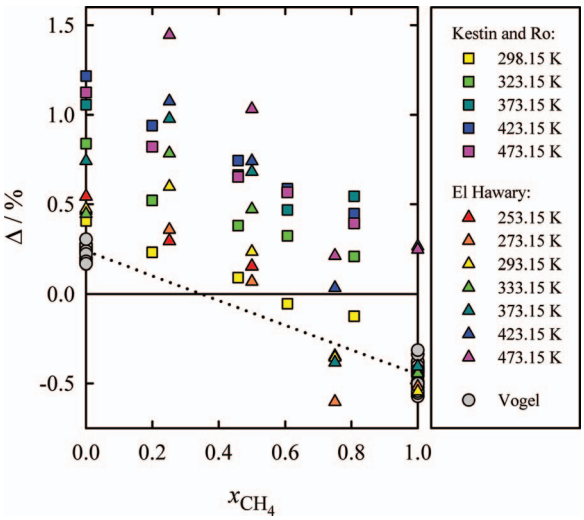

FIG. 5. Deviations, $\Delta = (\eta_{exp} - \eta_{cal})/\eta_{cal}$, of experimental viscosity data for dilute CH_4–N_2 mixtures and the pure components from values obtained with the adjusted potential function. The dotted line indicates the recommended values given by Eq. (18).

systematically too high above room temperature.[55] Thus, the uncertainty of their data at temperatures higher than room temperature is more likely to be around 1%. In principle, an exact comparison requires correcting these data for the initial density dependence of the viscosity. Since the Rainwater-Friend theory,[56,57] which deals with this dependence, has not been extended to gaseous mixtures, the correction has been estimated using the theory for the two pure gases. The viscosity values in the dilute-gas limit decrease roughly by 0.1%, nearly independent of temperature. In addition, all experimental data by Kestin's group were obtained in relative measurements based on a calibration, resulting in values that are $(0.1 - 0.2)$% too high compared with theoretically calculated ones, see, for example, Ref. 58. Considering the correction for the initial density dependence and a possible recalibration, the viscosity data of Kestin and Ro[53] are in excellent agreement with the calculated values at 298 K as illustrated in Fig. 5. At higher temperatures, as expected,[55] positive deviations of up to 1.2% from the calculated values are found.

Two rotating-cylinder viscometers, one for pressures up to 2.4 MPa and one for pressures up to 20 MPa, were used by El Hawary[54] to measure the viscosities of the pure components and three mixtures between 253 K and 473 K (only up to 373 K for pure nitrogen with the viscometer for low pressures). We extrapolated the viscosity data obtained with the viscometer for low pressures, for which a very low uncertainty estimate of 0.06% is given by El Hawary, to the limit of zero density. Based on the scatter of the data illustrated in Fig. 5 and on the comparison with reference values for the viscosity of the pure species (see below), together with the comparison with the values of Kestin and Ro[53] for the mixtures, we have no reason to believe that the uncertainty of El Hawary's data is any better than that of the data of Kestin and Ro. At the highest temperature it is most likely worse. Taking into account the proposed reassessed uncertainty of El Hawary's data, most of the extrapolated values are in good agreement with the computed ones, although some values at higher temperatures deviate by more than 1%.

Vogel measured the viscosities of pure methane[59] and pure nitrogen[60] at densities of less than 1 $\mathrm{kg\,m^{-3}}$ using an oscillating disk viscometer for temperatures between 292 K and 682 K. He derived values in the zero-density limit from the measured viscosities using the Rainwater-Friend theory. Vogel estimates the uncertainty of his values to be less than 0.2%. The deviations from our computed values are nearly independent of temperature and are on average +0.24% for nitrogen and −0.45% for methane. Hence, our best estimate for the shear viscosities of the pure gases is obtained by simply scaling the calculated values by 1.0024 and 0.9955 for nitrogen and methane, respectively. Assuming that for the mixtures the scaling factor depends linearly on the mole fraction, we arrive at the following correction for the calculated values:

$$\eta = \eta_{\mathrm{cal}}(1.0024 - 0.0069\, x_{\mathrm{CH_4}}). \tag{18}$$

The viscosities thus obtained are also indicated in Fig. 5. We estimate the uncertainty of these values to vary from 0.15% for pure nitrogen to 0.3% for pure methane in the temperature range of 300 K to 700 K, increasing to 1% at 70 K and 0.5% (pure nitrogen) to 1% (pure methane) at 1200 K. It is interesting to note that the deviations of the calculated values from the values of Kestin and Ro[53] and, to a certain extent, from El Hawary's[54] values follow a similar trend to that of Eq. (18), thus indicating that the deviations of the experimental data from the corrected viscosity values do not exhibit any systematic trend with composition.

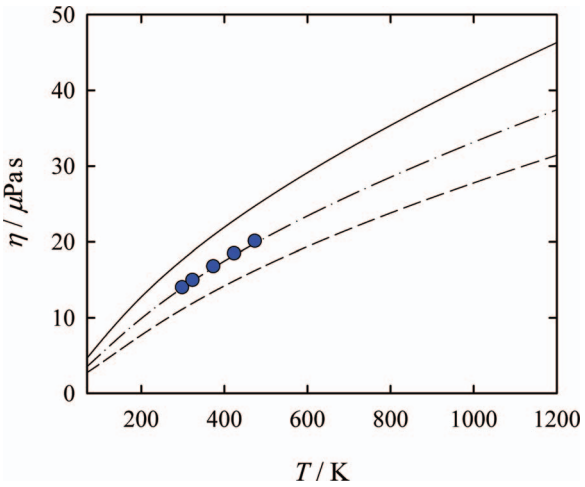

FIG. 6. Viscosity of pure nitrogen (——) and pure methane (– – –) in the first-order approximation, as well as interaction viscosity for the adjusted potential function (— · —). The circles represent interaction viscosity values obtained from the experimental data of Kestin and Ro (Ref. 53).

Figure 6 illustrates the behavior of the interaction viscosity, defined by Eq. (13), as a function of temperature. It exhibits a monotonic increase, and its value is within $(1 - 2)$% of the geometric mean of the viscosity values for the pure components in the first-order approximation, which are also shown. We also plotted the values of the interaction viscosity obtained from the experimental measurements by Kestin and Ro.[53] As no values are reported in the paper, we estimated them from the universal function given in the paper. The agreement is remarkably good, the deviations increasing from 0.9% at 298 K to 1.7% at the highest temperature measured (473 K). This indicates that for this particular mixture obtaining the interaction viscosity by analyzing measured viscosity values of the mixtures by means of the first-order theory and by using values of A^* obtained from spherical intermolecular potentials, which are on average (4–5)% lower, does not introduce appreciable errors. It remains to be seen if this is true for other mixtures. The values calculated for the interaction viscosity using Eq. (13) and for the pure-component viscosities in the first-order approximation can be found in the supplementary material.[34]

In Fig. 7, the binary diffusion coefficients computed with the adjusted potential function are compared with the experimental data of Wakeham and Slater[61] for a mixture with $x_{\mathrm{CH_4}} = 0.1$ at atmospheric pressure. Wakeham and Slater used the gas chromatographic method and estimated the uncertainty of their data to be (3–4)%. Apart from one datum, the deviations of the experimental data from the calculated values are within ±4%. We conservatively estimate the uncertainty of our calculated values to be 1% between 300 K and 700 K, increasing to 2% at both 70 K and 1200 K.

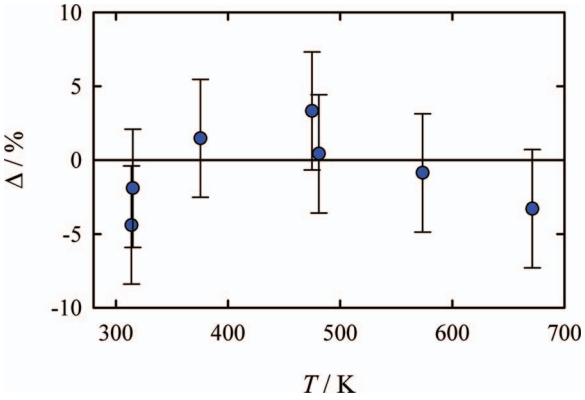

FIG. 7. Deviations, $\Delta = (\rho_m D_{exp} - \rho_m D_{cal})/\rho_m D_{cal}$, of the experimental values of Wakeham and Slater (Ref. 61) for the binary diffusion coefficient of a dilute CH_4–N_2 mixture with $x_{CH_4} = 0.1$ from the calculated values obtained with the adjusted potential function.

V. SUMMARY AND CONCLUSIONS

A new intermolecular potential energy surface for the CH_4–N_2 molecule pair was determined from quantum-chemical *ab initio* calculations. The counterpoise-corrected supermolecular approach at the CCSD(T) level of theory with basis sets of up to quadruple-zeta quality including bond functions was used to compute interaction energies for 743 geometries of the molecule pair. The potential energy surface was represented by an accurate analytical site-site potential function with nine sites for methane and five sites for nitrogen. It exhibits only one distinct equilibrium structure with a well depth of 237.54 K. In order to properly account for zero-point vibrational effects, the site-site potential function was adjusted by fitting to the most accurate experimental data for the cross second virial coefficient. The adjustment was achieved by increasing the strength of the C_8 dispersion contribution, resulting in a slightly larger well depth of 248.24 K for the equilibrium structure.

We have used the adjusted potential energy surface to calculate the cross second virial coefficient, shear viscosity, and binary diffusion coefficient of CH_4–N_2 gas mixtures and compared with the best experimental data. The cross second virial coefficient was computed using the Mayer-sampling Monte Carlo approach.[23] To account for quantum effects, the quadratic Feynman-Hibbs effective pair potential[43] was used in these calculations. The transport properties were computed using the classical trajectory method in conjunction with the kinetic theory of molecular gases.[1,24–30] The calculations were performed in the temperature range from 70 K to 1200 K, and the recommended vales are given for the cross second virial coefficient in Table I and for the transport properties in the supplementary material.[34] The thermal conductivity will be the subject of a separate publication.

The computed values of the cross second virial coefficient, shear viscosity, and binary diffusion coefficient, using the adjusted potential surface, are in good agreement with the experimental data, which are available only in the temperature range from 156 K to 671 K. We conservatively estimate the uncertainty of the calculated values for the cross second virial coefficient to vary from 14 cm^3 mol^{-1} at 70 K to 1 cm^3 mol^{-1} at 1200 K. For the viscosity of CH_4–N_2 mixtures, the uncertainty of the calculated values is estimated to vary from 0.15% for pure nitrogen between 300 K and 700 K to 1% for pure methane at 1200 K. For the binary diffusion coefficient, the corresponding uncertainty is estimated to vary between 1% and 2%.

In conclusion, the proposed potential energy surface for the CH_4–N_2 molecule pair has been validated against the best available thermophysical data, which are generally reproduced rather well, and the computed values provide reliable and accurate estimates of the cross second virial coefficient, shear viscosity, and binary diffusion coefficient. The calculation of transport properties of a mixture that contains two polyatomic species, reported here, is the first of its kind. The good agreement with the experimental data also indirectly offers the first accurate validation of the kinetic theory of polyatomic gas mixtures.

ACKNOWLEDGMENTS

This work was financially supported by the Deutsche Forschungsgemeinschaft (DFG), Grant No. BI 1389/1-1.

[1] F. R. W. McCourt, J. J. M. Beenakker, W. E. Köhler, and I. Kuščer, *Nonequilibrium Phenomena in Polyatomic Gases, Vol. I: Dilute Gases* (Clarendon Press, Oxford, 1990).
[2] R. Hellmann, E. Bich, and E. Vogel, J. Chem. Phys. **128**, 214303 (2008).
[3] R. Bukowski, K. Szalewicz, G. C. Groenenboom, and A. van der Avoird, J. Chem. Phys. **128**, 094313 (2008).
[4] R. Hellmann, E. Bich, E. Vogel, and V. Vesovic, Phys. Chem. Chem. Phys. **13**, 13749 (2011).
[5] G. Garberoglio, P. Jankowski, K. Szalewicz, and A. H. Harvey, J. Chem. Phys. **137**, 154308 (2012).
[6] R. Hellmann, Mol. Phys. **111**, 387 (2013).
[7] R. Hellmann, Chem. Phys. Lett. **613**, 133 (2014).
[8] J.-P. Crusius, R. Hellmann, E. Hassel, and E. Bich, J. Chem. Phys. **141**, 164322 (2014).
[9] R. Hellmann, E. Bich, E. Vogel, A. S. Dickinson, and V. Vesovic, J. Chem. Phys. **129**, 064302 (2008).
[10] R. Hellmann, E. Bich, E. Vogel, A. S. Dickinson, and V. Vesovic, J. Chem. Phys. **130**, 124309 (2009).
[11] R. Hellmann, E. Bich, E. Vogel, A. S. Dickinson, and V. Vesovic, J. Chem. Phys. **131**, 014303 (2009).
[12] A.-M. Harri, T. Mäkinen, A. Lehto, H. Kahanpää, and T. Siili, Planet. Space Sci. **54**, 1117 (2006).
[13] A. Heintz and E. Bich, Pure Appl. Chem. **81**, 1903 (2009).
[14] G. Firanescu, D. Luckhaus, G. N. Patey, S. K. Atreya, and R. Signorell, Icarus **212**, 779 (2011).
[15] A. Petculescu and P. Achi, J. Acoust. Soc. Am. **131**, 3671 (2012).
[16] C. R. Glein and E. L. Shock, Geochim. Cosmochim. Acta **115**, 217 (2013).
[17] H. Schindler, R. Vogelsang, V. Staemmler, M. A. Siddiqi, and P. Svejda, Mol. Phys. **80**, 1413 (1993).
[18] M. Shadman, S. Yeganegi, and F. Ziaie, Chem. Phys. Lett. **467**, 237 (2009).
[19] T. H. Dunning, Jr., J. Chem. Phys. **90**, 1007 (1989).
[20] R. A. Kendall, T. H. Dunning, Jr., and R. J. Harrison, J. Chem. Phys. **96**, 6796 (1992).
[21] Y. N. Kalugina, V. N. Cherepanov, M. A. Buldakov, N. Zvereva-Loëte, and V. Boudon, J. Chem. Phys. **131**, 134304 (2009).
[22] K. Raghavachari, G. W. Trucks, J. A. Pople, and M. Head-Gordon, Chem. Phys. Lett. **157**, 479 (1989).
[23] J. K. Singh and D. A. Kofke, Phys. Rev. Lett. **92**, 220601 (2004).
[24] L. Waldmann, "Transporterscheinungen in Gasen von mittlerem Druck," in *Handbuch der Physik*, edited by S. Flügge (Springer-Verlag, Berlin, 1958), Vol. 12, pp. 295–514.
[25] L. Waldmann and E. Trübenbacher, Z. Naturforsch. **17a**, 363 (1962).
[26] J. H. Ferziger and H. G. Kaper, *The Mathematical Theory of Transport Processes in Gases* (North-Holland, Amsterdam, 1972).
[27] C. F. Curtiss, J. Chem. Phys. **75**, 1341 (1981).

[28]M. Mustafa, "Measurement and calculation of transport properties of polyatomic gases," Ph.D. thesis, Imperial College London, London, UK, 1987.
[29]E. L. Heck and A. S. Dickinson, Comput. Phys. Commun. **95**, 190 (1996).
[30]A. S. Dickinson, R. Hellmann, E. Bich, and E. Vogel, Phys. Chem. Chem. Phys. **9**, 2836 (2007).
[31]A. K. Dham, F. R. W. McCourt, and A. S. Dickinson, J. Chem. Phys. **127**, 054302 (2007).
[32]E. Bich, J. B. Mehl, R. Hellmann, and V. Vesovic, in *Experimental Thermodynamics Volume IX: Advances in Transport Properties of Fluids*, edited by M. J. Assael, A. R. H. Goodwin, V. Vesovic, and W. A. Wakeham (The Royal Society of Chemistry, Cambridge, 2014), Chap. 7, pp. 226–252.
[33]R. Hellmann and E. Bich, "An improved kinetic theory approach for calculating the thermal conductivity of polyatomic gases," Mol. Phys. (published online).
[34]See supplementary material at http://dx.doi.org/10.1063/1.4902807 for details of the Euler angles used, the parameters and the equilibrium structure of the analytical potential function, results of the *ab initio* calculations for all 743 points on the PES, and tables of the transport property values calculated in this work.
[35]S. F. Boys and F. Bernardi, Mol. Phys. **19**, 553 (1970).
[36]A. Halkier, T. Helgaker, P. Jørgensen, W. Klopper, H. Koch, J. Olsen, and A. K. Wilson, Chem. Phys. Lett. **286**, 243 (1998).
[37]J. F. Stanton, J. Gauss, J. D. Watts, P. G. Szalay, R. J. Bartlett with contributions from A. A. Auer, D. E. Bernholdt, O. Christiansen, M. E. Harding, M. Heckert, O. Heun, C. Huber, D. Jonsson, J. Jusélius, W. J. Lauderdale, T. Metzroth, C. Michauk, D. R. Price, K. Ruud, F. Schiffmann, A. Tajti, M. E. Varner, J. Vázquez and the integral packages: *MOLECULE* (J. Almlöf and P. R. Taylor), *PROPS* (P. R. Taylor), and *ABACUS* (T. Helgaker, H. J. Aa. Jensen, P. Jørgensen, and J. Olsen). See also J. F. Stanton, J. Gauss, J. D. Watts, W. J. Lauderdale, and R. J. Bartlett, Int. J. Quantum Chem. Symp. 26, 879–894 (1992). Current version see http://www.aces2.de.
[38]CFOUR, Coupled-Cluster techniques for Computational Chemistry, a quantum-chemical program package by J. F. Stanton, J. Gauss, M. E. Harding, P. G. Szalay with contributions from A. A. Auer, R. J. Bartlett, U. Benedikt, C. Berger, D. E. Bernholdt, Y. J. Bomble, L. Cheng, O. Christiansen, M. Heckert, O. Heun, C. Huber, T.-C. Jagau, D. Jonsson, J. Jusélius, K. Klein, W. J. Lauderdale, D. A. Matthews, T. Metzroth, L. A. Mück, D. P. O'Neill, D. R. Price, E. Prochnow, C. Puzzarini, K. Ruud, F. Schiffmann, W. Schwalbach, S. Stopkowicz, A. Tajti, J. Vázquez, F. Wang, J. D. Watts and the integral packages molecule (J. Almlöf and P. R. Taylor), props (P. R. Taylor), abacus (T. Helgaker, H. J. Aa. Jensen, P. Jørgensen, and J. Olsen), and ECP routines by A. V. Mitin and C. van Wüllen. For the current version, see http://www.cfour.de.
[39]K. T. Tang and J. P. Toennies, J. Chem. Phys. **80**, 3726 (1984).
[40]D. J. Margoliash and W. J. Meath, J. Chem. Phys. **68**, 1426 (1978).
[41]A. J. Russell and M. A. Spackman, Mol. Phys. **84**, 1239 (1995).
[42]D. M. Bishop, F. L. Gu, and S. M. Cybulski, J. Chem. Phys. **109**, 8407 (1998).
[43]R. P. Feynman and A. R. Hibbs, *Quantum Mechanics and Path Integrals* (McGraw-Hill, New York, 1965).
[44]B. Jäger, R. Hellmann, E. Bich, and E. Vogel, J. Chem. Phys. **135**, 084308 (2011).
[45]D. R. Roe, "Thermodynamic properties of gases and gas mixtures at low temperatures and high pressures," Ph.D. thesis, Imperial College, London, UK, 1972.
[46]M. L. Martin, R. D. Trengove, K. R. Harris, and P. J. Dunlop, Aust. J. Chem. **35**, 1525 (1982).
[47]M. Jaeschke and M. Hinze, *Ermittlung des Realgasverhaltens von Methan und Stickstoff und deren Gemische im Temperaturbereich von 270 K bis 353 K und Drücken bis 30 MPa*, Fortschr.-Ber. VDI, Reihe 3, Nr. 262 (VDI-Verlag, Düsseldorf, 1991).
[48]B. D. Ababio, P. J. McElroy, and C. J. Williamson, J. Chem. Thermodyn. **33**, 413 (2001).
[49]G. C. Maitland, M. Rigby, E. B. Smith, and W. A. Wakeham, *Intermolecular Forces: Their Origin and Determination* (Clarendon Press, Oxford, 1987).
[50]S. Bock, E. Bich, E. Vogel, A. S. Dickinson, and V. Vesovic, J. Chem. Phys. **117**, 2151 (2002).
[51]R. Hellmann, E. Bich, E. Vogel, and V. Vesovic, J. Chem. Eng. Data **57**, 1312 (2012).
[52]R. Hellmann, N. Riesco, and V. Vesovic, J. Chem. Phys. **138**, 084309 (2013).
[53]J. Kestin and S. T. Ro, Ber. Bunsenges. Phys. Chem. **78**, 20 (1974).
[54]T. El Hawary, "Messung der Dichte und Viskosität in der Gasphase von Methan, Stickstoff und Methan-Stickstoff-Gemischen mit einer weiterentwickelten kombinierten Viskositäts-Dichte-Messanlage und einer neuen Viskositätsmessanlage für geringe Gasdichten," Ph.D. thesis, Ruhr-Universität Bochum, Bochum, Germany, 2009.
[55]E. Vogel, C. Küchenmeister, E. Bich, and A. Laesecke, J. Phys. Chem. Ref. Data **27**, 947 (1998).
[56]J. C. Rainwater and D. G. Friend, Phys. Rev. A **36**, 4062 (1987).
[57]E. Bich, and E. Vogel, in *Transport Properties of Fluids*, edited by J. Millat, J. H. Dymond, and C. A. Nieto de Castro (Cambridge University Press, Cambridge, 1996), Chap. 5.2, pp. 72–82.
[58]E. Vogel, B. Jäger, R. Hellmann, and E. Bich, Mol. Phys. **108**, 3335 (2010).
[59]E. Vogel, J. Chem. Eng. Data **56**, 3265 (2011).
[60]E. Vogel, Int. J. Thermophys. **33**, 741 (2012).
[61]W. A. Wakeham and D. H. Slater, J. Phys. B **6**, 886 (1973).